Electronics Letters

Special issue
Call for Papers

Be Seen. Be Cited.
Submit your work to a new IET special issue

Connect with researchers and experts in your field and share knowledge.

Be part of the latest research trends, faster.

Read more

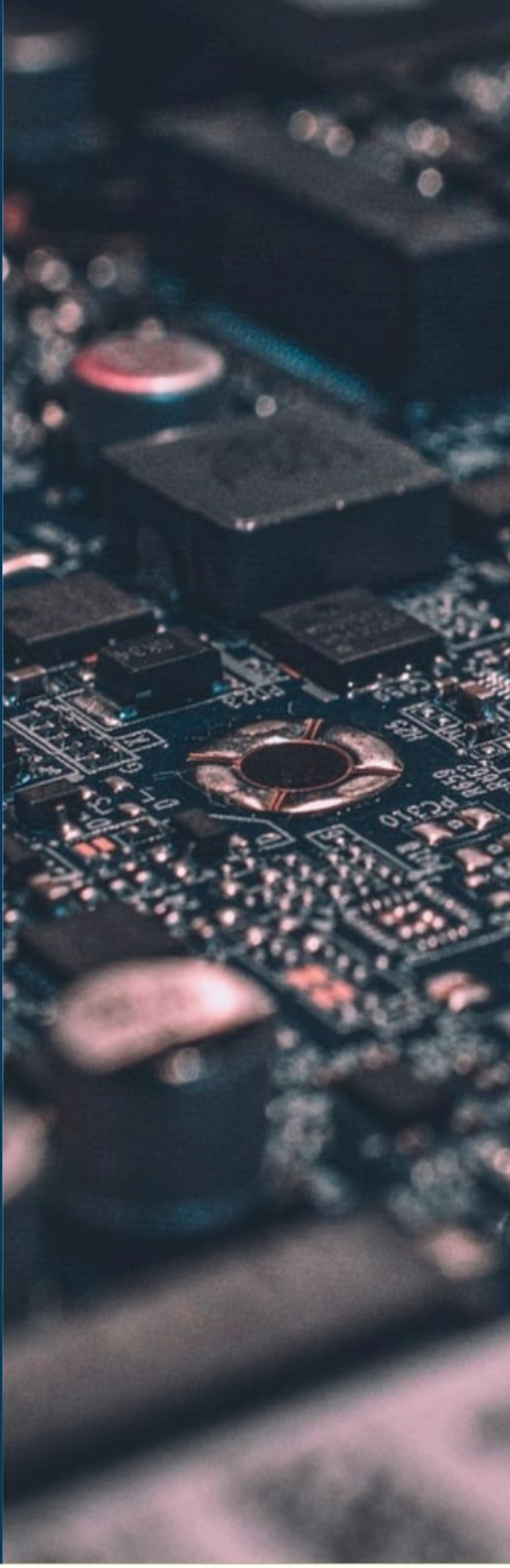

The Institution of Engineering and Technology

Six-port QPSK demodulator for optimal K-band multiport amplifier calibration

Han Lim Lee, Seong-Mo Moon, Moon-Que Lee and Jong Won Yu

A wideband six-port-based demodulator is proposed and applied as a quadrature phase shift keying (QPSK) demodulator for optimal K-band multiport amplifier (MPA) calibration circuitry. The proposed six-port demodulator adopts wideband ring hybrids for optimal 180° phase balance in local oscillator signal paths. In addition, a voltage-controlled reflection-type phase shifter and an attenuator are integrated into the six-port structure to ensure accurate magnitude and phase balance over broadband operation, resulting in optimal phase and amplitude error detection for the MPA system. To verify the proposed structure, RF demodulation of the K-band QPSK modulated signal was demonstrated for purpose of MPA calibration.

Introduction: Although the multiport amplifier (MPA) has become an attractive solution due to its advantages of power flexibility and lower DC power consumption compared to conventional amplification structures [1], different electrical characteristics in each signal path of the MPA can cause poor isolation among channels, resulting in degradation of the system performance. Thus, several calibration techniques have been proposed to achieve high port-to-port isolation [2, 3] and the most up-to-date calibration technique was introduced in [3]. The calibration technique in [3] detects amplitude and phase errors distinctively, and then performs calibration through axial ratio comparisons. That is, a high-performance quadrature phase shift keying (QPSK) demodulator that can precisely reproduce the amplitude and phase errors from RF signal paths into baseband signals for optimal error correction is required.

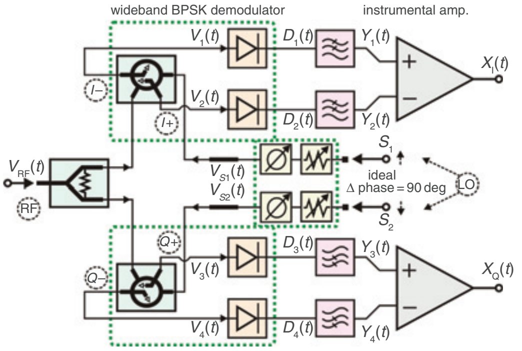

Fig. 1 *Schematic of proposed six-port-based demodulator for optimal K-band MPA calibration*

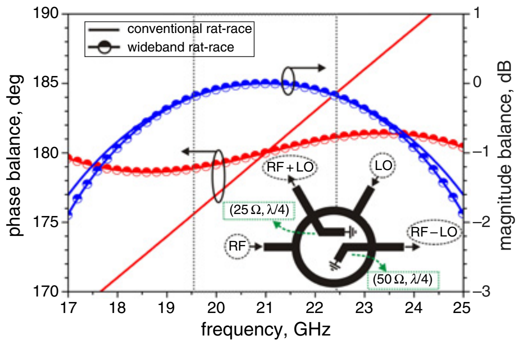

Fig. 2 *Comparison of simulated wideband and conventional ring hybrid*

Design and analysis: Fig. 1 shows the proposed wideband six-port QPSK demodulator which ensures no additional amplitude and phase imbalances that can corrupt the original amplitude and phase errors of MPA signal paths. To optimally correct MPA signal path errors, the local oscillator (OL) signal paths of the QPSK demodulator must be accurately balanced such that each ring hybrid should operate as an ideal binary phase shift keying (BPSK) demodulator. For K-band operation (19.5–22.5 GHz), wideband ring hybrids, voltage-controlled phase shifters and attenuators are adopted for optimal QPSK signal balance, resulting in optimal correction of MPA signal path errors. Compared to the conventional ring hybrid, the wideband ring hybrid modified from [4] has excellent magnitude and phase balances in the operation band as shown in Fig. 2.

The modulated RF signal and the LO signals to be sampled from MPA signal paths are defined as

$$V_{\mathrm{RF}}(t) = 2A_{\mathrm{RF}}\cos(2\pi f_{\mathrm{RF}}t + \phi(t)) \tag{1}$$

$$V_{\mathrm{LO}}(t) = A_{\mathrm{LO}}\cos(2\pi f_{\mathrm{LO}}t) \tag{2}$$

where $\phi(t)$ implies phase modulation. Then, S_1 and S_2 represent the sampled signals including amplitude and phase errors from MPA signal paths as follows:

$$S_1(t) = \alpha_A A_{\mathrm{LO}}\cos(2\pi f_{\mathrm{LO}}t + \theta_A) \tag{3}$$

$$S_2(t) = \alpha_B A_{\mathrm{LO}}\cos(2\pi f_{\mathrm{LO}}t + \pi/2 + \theta_B) \tag{4}$$

where $\alpha_{A,B}$ and $\theta_{A,B}$ indicate the amplitude and phase errors of MPA signal paths. Since the proposed six-port architecture has a voltage-controlled phase shifter and attenuator, control voltage dependent amplitude and phase variation factors, $\alpha_{M,N}(v)$ and $\theta_{M,N}(v)$, are added as shown in (5) and (6)

$$V_{S1}(t) = (\alpha_A + \alpha_M(v))A_{\mathrm{LO}}\cos(2\pi f_{\mathrm{LO}}t + \theta_A + \theta_M(v)) \tag{5}$$

$$V_{S2}(t) = (\alpha_B + \alpha_N(v))A_{\mathrm{LO}}\cos(2\pi f_{\mathrm{LO}}t + \pi/2 + \theta_B + \theta_N(v)) \tag{6}$$

For the conventional six-port architecture, $\alpha_{M,N}(v)$ and $\theta_{M,N}(v)$ would be 0. After the RF signal and LO signals are mixed through a Wilkinson divider and wideband ring hybrids, the signals can be expressed as follows:

$$\begin{aligned} V_1(t) = {} & (\alpha_A + \alpha_M(v) + \alpha_1)A_{\mathrm{LO}}\cos(2\pi f_{\mathrm{LO}}t + \theta_A \\ & + \theta_M(v) + \theta_i) + \beta A_{\mathrm{RF}}\cos(2\pi f_{\mathrm{RF}}t + \phi(t)) \end{aligned} \tag{7}$$

$$\begin{aligned} V_2(t) = {} & (\alpha_A + \alpha_M(v) + \alpha_2)A_{\mathrm{LO}}\cos(2\pi f_{\mathrm{LO}}t + \theta_A \\ & + \theta_M(v) + \theta_i + \Delta\theta_i) + \beta A_{\mathrm{RF}}\cos(2\pi f_{\mathrm{RF}}t + \phi(t)) \end{aligned} \tag{8}$$

$$\begin{aligned} V_3(t) = {} & (\alpha_B + \alpha_N(v) + \alpha_3)A_{\mathrm{LO}}\cos(2\pi f_{\mathrm{LO}}t + \pi/2 + \theta_B + \theta_N(v) + \theta_j) \\ & + \beta A_{\mathrm{RF}}\cos(2\pi f_{\mathrm{RF}}t + \phi(t)) \end{aligned} \tag{9}$$

$$\begin{aligned} V_4(t) = {} & (\alpha_B + \alpha_N(v) + \alpha_4)A_{\mathrm{LO}}\cos(2\pi f_{\mathrm{LO}}t + \pi/2 + \theta_B + \theta_N(v) + \theta_j \\ & + \Delta\theta_j) + \beta A_{\mathrm{RF}}\cos(2\pi f_{\mathrm{RF}}t + \phi(t)) \end{aligned} \tag{10}$$

where $\alpha_{1,2,3,4}$ denotes the additional loss by the wideband ring hybrid. θ_i and θ_j denote the relative phases at one output port of each upper and lower ring hybrid, respectively. In addition, $\triangle\theta_i$ and $\triangle\theta_j$ denote the relative phase balances between two output ports of each upper and lower ring hybrid, respectively. Lastly, β indicates the amplitude attenuation in the RF signal by the six-port-based architecture and is assumed to be constant since the signal is divided equally over the operation band. By adopting the wideband ring hybrid whose electrical performance is described in Fig. 2, $\alpha_1 = \alpha_2 = \alpha_{\mathrm{U}}$, $\alpha_3 = \alpha_4 = \alpha_{\mathrm{L}}$ and $\triangle\theta_i = \triangle\theta_j = \pi$ can be achieved in the operation band. In addition, since the voltage-controlled attenuator and phase shifter are added, $\alpha_M(v) + \alpha_{\mathrm{U}} = \alpha_N(v) + \alpha_{\mathrm{L}} = \alpha$ and $\theta_M(v) + \theta_i = \theta_N(v) + \theta_j = \theta$ can be achieved by properly adjusting the control voltages of the attenuators and phase shifters. That is, optimal demodulator operation for the K-band MPA calibration process can be obtained by ensuring the accurate amplitude and phase errors, α_A, α_B, θ_A and θ_B. After the wideband six-port-based structure is fine-tuned by the phase shifter and attenuator, (7)–(10) can be simplified as below

$$\begin{aligned} V_K(t)\big|_{K=1,2} = {} & (\alpha_A + \alpha)A_{\mathrm{LO}}\cos(2\pi f_{\mathrm{LO}}t + \theta_A + \theta_K) \\ & + \beta A_{\mathrm{RF}}\cos(2\pi f_{\mathrm{RF}}t + \phi(t)) \end{aligned} \tag{11}$$

$$\begin{aligned} V_K(t)\big|_{K=3,4} = {} & (\alpha_B + \alpha)A_{\mathrm{LO}}\cos(2\pi f_{\mathrm{LO}}t + \theta_A + \theta_K) \\ & + \beta A_{\mathrm{RF}}\cos(2\pi f_{\mathrm{RF}}t + \phi(t)) \end{aligned} \tag{12}$$

where relative phases are $\theta_1 = 0$, $\theta_2 = \pi$, $\theta_3 = \pi/2$ and $\theta_4 = 3\pi/2$. Then, by diode detectors, $V_K(t)\ /_{K=1,2}$ signals are converted as follows:

$$\begin{aligned} D_K(t)\big|_{K=1,2} = {} & K[(\alpha_A + \alpha)A_{\mathrm{LO}}\cos(2\pi f_{\mathrm{LO}}t + \theta_A + \theta_K) \\ & + \beta A_{\mathrm{RF}}\cos(2\pi f_{\mathrm{RF}}t + \phi(t))]^2 \end{aligned} \tag{13}$$

By lowpass filtering (13) and applying $f_{\mathrm{RF}} = f_{\mathrm{LO}}$ for direction conversion, (14) and (15) can be achieved. Similarly, (16) and (17) can be derived from $V_K(t)|_{K=3,4}$

$$Y_1(t)\big|_{\theta_1=0} = \frac{K(\alpha_A+\alpha)^2A_{\mathrm{LO}}^2}{2} + \frac{K\beta^2A_{\mathrm{RF}}^2}{2} + K(\alpha_A+\alpha)\beta A_{\mathrm{LO}}A_{\mathrm{RF}}\cos(0-(\theta_A+\phi(t))) \tag{14}$$

$$Y_2(t)\big|_{\theta_2=\pi} = \frac{K(\alpha_A+\alpha)^2A_{\mathrm{LO}}^2}{2} + \frac{K\beta^2A_{\mathrm{RF}}^2}{2} + K(\alpha_A+\alpha)\beta A_{\mathrm{LO}}A_{\mathrm{RF}}\cos(\pi-(\theta_A+\phi(t))) \tag{15}$$

$$Y_3(t)\big|_{\theta_3=\pi/2} = \frac{K(\alpha_B+\alpha)^2A_{\mathrm{LO}}^2}{2} + \frac{K\beta^2A_{\mathrm{RF}}^2}{2} + K(\alpha_B+\alpha)\beta A_{\mathrm{LO}}A_{\mathrm{RF}}\cos(\pi/2-(\theta_B+\phi(t))) \tag{16}$$

$$Y_4(t)\big|_{\theta_4=3\pi/2} = \frac{K(\alpha_B+\alpha)^2A_{\mathrm{LO}}^2}{2} + \frac{K\beta^2A_{\mathrm{RF}}^2}{2} + K(\alpha_B+\alpha)\beta A_{\mathrm{LO}}A_{\mathrm{RF}}\cos(3\pi/2-(\theta_B+\phi(t))) \tag{17}$$

Using instrumental amplifiers to eliminate DC-offsets, I and Q signals can finally be obtained as follows:

$$X_I(t) = Y_1(t) - Y_2(t) = 2\,K(\alpha_A+\alpha)\beta A_{\mathrm{LO}}A_{\mathrm{RF}}\cos(\theta_A+\phi(t)) \tag{18}$$

$$X_Q(t) = Y_3(t) - Y_4(t) = 2\,K(\alpha_B+\alpha)\beta A_{\mathrm{LO}}A_{\mathrm{RF}}\sin(\theta_B+\phi(t)) \tag{19}$$

According to (18) and (19), the relative amplitude and phase imbalance among the signal paths of the MPA, $|\alpha_A - \alpha_B|$ and $|\theta_A - \theta_B|$, can be accurately compared, resulting in optimal amplitude and phase calibration in the MPA.

Measurement results: For the proposed demodulator, wideband ring hybrids, phase shifters and attenuators were implemented by monolithic microwave integrated circuit in the 0.15 µm GaAs low noise high-electron-mobility transistor [pHEMT] process. The measured maximum phase shift of 80° and the insertion loss variation $< \pm 0.1$ dB were obtained by the phase shifter in the operation band. The attenuator also showed the measured maximum attenuation of 7 dB and a phase variation of $< \pm 1°$. Fig. 3 shows the implemented K-band six-port-based QPSK demodulator for the MPA calibration. To verify the proposed structure, the pseudorandom QPSK data stream with 10 Mbit/s data rate for RF was applied using a vector signal generator where high data rate was not necessary for purpose of calibration. In addition, continuous-wave signals for LO were applied using a high-frequency signal generator through a K-band waveguide branch-line coupler for 90° phase difference. Then, the demodulated signals were directly analysed using a mixed signal oscilloscope. Finally, the successful demodulation performance of the proposed structure at 21 GHz is shown in Fig. 3.

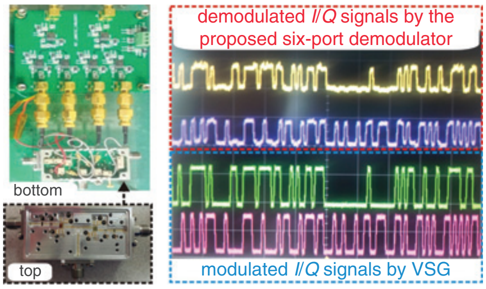

Fig. 3 *Measured results for proposed six-port-based demodulator*

Conclusion: A wideband six-port-based QPSK demodulator for optimal K-band MPA calibration is proposed. For optimal amplitude and phase error correction of the most up-to-date MPA calibration [3], a high-performance QPSK demodulator is necessary in order to accurately retrieve amplitude and phase error information in the baseband. Since wideband ring hybrids, tunable phase shifters and attenuators are integrated as a six-port demodulator, the proposed architecture can be optimally used for K-band MPA calibration.

Acknowledgment: This research was supported by the Basic Science Research Program through the National Research Foundation of Korea (NRF) funded by the Ministry of Science, ICT & Future Planning (2012R1A1A2008310).

© The Institution of Engineering and Technology 2014

13 January 2014
doi: 10.1049/el.2013.4147
One or more of the Figures in this Letter are available in colour online.

Han Lim Lee and Jong Won Yu (*Department of Electrical Engineering, KAIST, 291 Daehak-ro, Yuseong-gu, Daejeon 305-701, Republic of Korea*)

Seong-Mo Moon (*RF and Satellite Payload Research Team, ETRI, 138 Gajeong-ro, Yuseong-gu, Daejeon 305-700, Republic of Korea*)

Moon-Que Lee (*Department of Electrical and Computer Engineering, University of Seoul, Siripdae-Gil 13, Dongdaemun-gu, Seoul 130-743, Republic of Korea*)

E-mail: mqlee@uos.ac.kr

References

1 Mallet, A., Anakabe, J., Sombrin, J., and Rodriguez, R.: ‘Multiport-amplifier based architecture versus classical architecture for space telecommunication payloads’, *IEEE Trans. Microw. Theory Tech.*, 2006, **54**, (12), pp. 4353–4361
2 Zhu, Z., Huang, X., and Caron, M.: ‘Ka-band multi-port power amplifier calibration experiment and results’. 2nd Int. Conf. Advances in Satellite Space Communications, Athens, Greece, June, 2010, pp. 11–14
3 Moon, S.-M., Shin, D.-H., Lee, H.-Y., Yom, I.-B., and Lee, M.-Q.: ‘Adaptive calibration method in multiport amplifier for K-band payload applications’, *ETRI J.*, 2013, **35**, (4), pp. 718–721
4 Na, W., Song, J., Cho, I.-H., Ryu, K.-K., and Lee, M.-Q.: ‘Ring hybrid balun with good amplitude and phase balance’. IEEE Microwave Symp. Dig., Hawaii, June, 2007

1350911x, 2014, 8, Downloaded from https://ietresearch.onlinelibrary.wiley.com/doi/10.1049/el.2013.4147 by Chung-Ang University, Wiley Online Library on [17/09/2023]. See the Terms and Conditions (https://onlinelibrary.wiley.com/terms-and-conditions) on Wiley Online Library for rules of use; OA articles are governed by the applicable Creative Commons License